TENTH AUSTRALASIAN FLUID MECHANICS
CONFERENCE - UNIVERSITY OF MELBOURNE
11-15 DECEMBER 1989

REDUCTION OF SOUND GENERATED BY A PLANE JET IMPINGING ON A CIRCULAR CYLINDER

Osamu MOCHIZUKI and Masaru KIYA

Faculty of Engineering
Hokkaido University
Sapporo, 060
JAPAN

ABSTRACT

Sound generated by a plane jet impinging on a circular cylinder was found to be significantly reduced by making a groove in the cylinder, which was filled with a low acoustic admittance material. This groove was located at a position where vorties in the jet impinge on the cylinder. In order to have high reduction the depth of the groove should be equal to a quarter of the wave length of the pressure fluctuation induced by the vortices of the impinging jet. Acoustic intensity vector field around the cylinder showed that the pressure fluctuation due to the impinging vortices does not produce pressure wave propagating upstream to maintain the feedback mechanism of self-sustained oscillating flows. The propagating pressure was suggested to be associated with vortices shed from the cylinder.

INTRODUCTION

A pure-tone sound is generated by a rigid circular cylinder placed near a two-dimensional nozzle, the axis of the cylinder being parallel to the nozzle. Mochizuki, Kiya and Tazumi(1987) showed that the magnitude and frequency of the sound depend on the diameter of the cylinder and the distance between the nozzle and the cylinder if the velocity at the exit of the nozzle is the same. The relation between the frequency and the distance was found to be the same as that for the edge tone. Thus the jet impinging on the circular cylinder forms a kind of self-excited oscillating flows.

Ho and Nosseir(1981) obtained details of the feedback mechanism of the jet impinging on a normal plate. They showed that disturbances propagating in the upstream direction are pressure fluctuations in the impingement region. Kaykayogle and Rockwell(1985,1986) investigated relations between the vortices and surface pressure fluctuations at the tip of the wedge placed in the jet. They showed that a secondary vortex induced by the jet vortices gives rise to a maximum amplitude of the surface pressure. However, exact relations between the sound produced by the self-excited flows and the surface pressures in the impingement region still remain to be clarified.

The purpose of this paper is 1) to obtain the relation between the pressure fluctuations propagating upstream and the surface-pressure fluctuations in the impingement region, and 2) to reduce the sound produced by the self-excited oscillating flow by preventing the upstream propagation of the pressure fluctuations. Cross correlations of pressure fluctuations on the cylinder surface and in space were measured, together with instantaneous flow fields obtained by a conditional flow- visualization technique combined with a pressure fluctuation waveform at a fixed point. The acoustic intensity vectors were obtained by the two-microphone sound intensity measurement technique. Based on these experimental results, a means to reduce the sound from the self-excited oscillating flow was obtained.

2 EXPERIMENTAL APPARATUS AND METHOD

Experiments were carried out in an anechoic chamber of dimensions $2.3*2.0*3.3m^2$ in which the jet flow was virtually free from any noise from the blower. A rectangular nozzle 15mm in height (H), 240mm in width and a circular cylinder 30mm in diameter (D), 350mm long are illustrated in Fig. 1 together with the definition of main symbols. The cylinder was set at a position $x_e/H=4.8$, where the sound attained a maximum intensity. Here, x_e is the distance between the nozzle and the front stagnation point of the cylinder. The velocity at the nozzle exit is denoted by U_0. Angle measured from a front stagnation point in the clockwise direction is written as θ. Point A ($x=4.8H, y=20.0H$) is a fixed position where the pressure fluctuation (hereinafter denoted by near-field pressure fluctuation: NFPF) was measured by a piezo microphone. This pressure waveform was employed as a reference signal. The surface-pressure fluctuations at different angles were measured by a semi-conductor strain-gauged pressure transducer mounted inside the cylinder. The acoustic intensity vectors were obtained by means of the two-microphone cross-spectral method presented by Waser and Crocker(1984). Pressure signals were measured by two piezo microphones 5.6mm in outer diameter. The two microphones were arranged side by side 10mm apart to avoid a near-field error greater than 1dB. The acoustic intensity was computed from the pressure signals detected by the two microphones by a dual FFT processor. The error of the acoustic intensity measured by this system was less than 3% for sound with a frequency 270Hz, which was the dominant frequency of the flow field of this study.

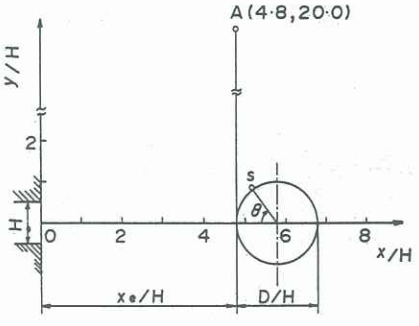

Fig. 1 Experimental setup and definition of symbols.

In order to obtain instantaneous flow fields, flow visualizations were performed with a smoke-wire method at an arbitrary phase of the NFPF. Moreover, to obtain vorticity distributions in the flow at an arbitrary phase of the NFPF, the velocity components u,v in the x,y directions respectively, were measured by split-film probes and phase-averaged. The vorticity component in the direction normal to the xy-plane ω was caluculated from $\omega=(d\langle v\rangle/dx-d\langle u\rangle/dy)D/U_0$, where U_c is the average convection velocity of the vortices.

3. RESULTS AND DISCUSSION

Unless otherwise stated, Reynolds number $Re(=U_0D/\nu$, ν: the kinematic viscosity) was 4.7×10^4, U_0 being 44m/s. The fundamental frequency f_0 of the NFPF was 270Hz.

3.1 Instantaneous flow field

Figure 2 shows the instantaneous flow fields in terms of the vorticity contours at the maximum (iii) and minimum (vii) of the NFPF detected at point A. Shaded regions are isolated regions of vorticity higher than $\omega=0.6$. A high-vorticity region first appears near the cylinder at phase (v); this can be interpreted as a large-scale vortex in the jet. At phase (vii), the large-scale vortex exists near the surface of the cylinder at a position $\theta=50$ degrees. At phase (iii), a vortex pair which consists of the large-scale vortex and the induced vortex with the opposite sense of vorticity (represented by broken lines) is shed from the cylinder. The large-scale vortex and the induced vortex seem to be formed, being synchronized with the NFPF, since the frequency of shedding of the vortex pair from one side of the cylinder is exactly equal to the dominant frequency of the NFPF.

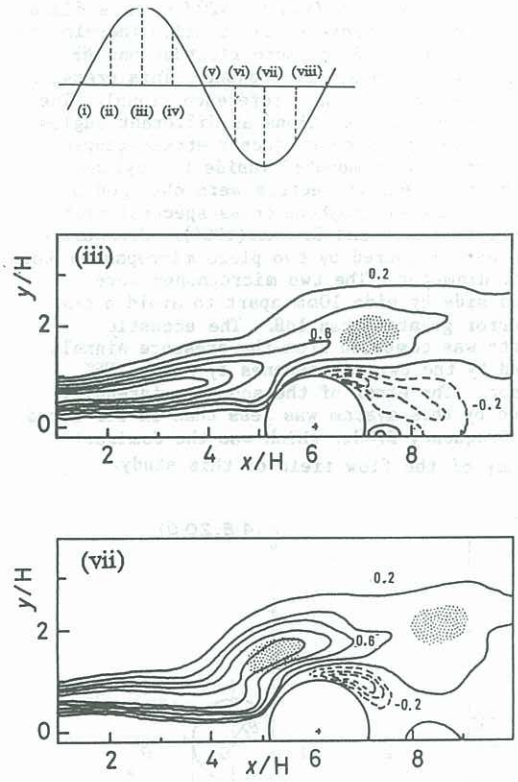

Fig. 2 Vorticity distributions at maximum and minimum of NFPF. Contour interval is 0.2. Shaded regions are isolated regions of vorticity higher than $\omega=0.6$.

Fig. 3 Instantaneous flow pattern at phase (vii) visualized by smoke.

Figure 3 shows the large-scale vortex and the induced vortex at phase (vii) visualized by smoke. The large-scale vortex consists of multiple vortices (three vortices in this figure), which have rolled up due to the Kelvin-Helmholtz instability. These vortices will hereinafter be refered to as K-H vortices. This is similar to the mechanism of formation of a coherent structure in the excited shear layer (Ho and Huang 1982). On the other hand, the induced vortex near the separation point seems to be produced by gradual accumulation of vorticity.

3.2 Relation between NFPF and surface pressure

The r.m.s. pressure coefficient $Cp'(=(\overline{p'^2})^{1/2}/\rho U_0/2$, p' being pressure fluctuation on the surface)is shown in Fig. 4. The r.m.s. pressure attains maximum at $\theta=50$ degrees, where the large-scale vortices of the jet impinge, as shown in Fig. 2. This position will hereinafter be refered to as impinging point: IP. The dominant frequency of the surface-pressure fluctuation at the IP was 270Hz, which is equal to that of the NFPF. Minor peaks appear at about $\theta=\pm120$ degrees, which correspond to the separation point associate with the induced vortices.

Figure 5 shows the cross correlation coefficient $R_a(\theta,t)$ of the pressure fluctuation on the surface and that at the point A, and the time lag t when R_a attains a maximum. The cross correlation is unity in a range $\theta=30$–90 degrees. On the other hand, the time lag t for $\theta=30$–90 degrees increases linearly with increasing angle θ. The gradient of the straight line in Fig. 5(b) is the convection velocity of the large-scale vortex in the jet. Since the large-scale vortex is near the surface in a range $\theta=30$–90 degrees (See phases (v)–(viii) in Fig. 2), the above results demonstrate that the surface-pressure fluctuation is strongly related to the large-scale vortex.

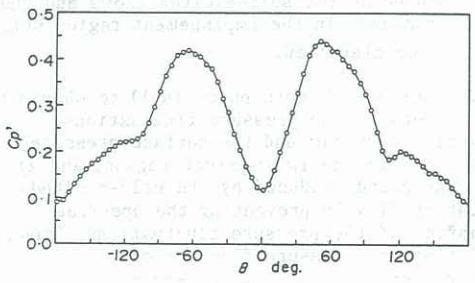

Fig. 4 R.m.s. surface-pressure coefficient.

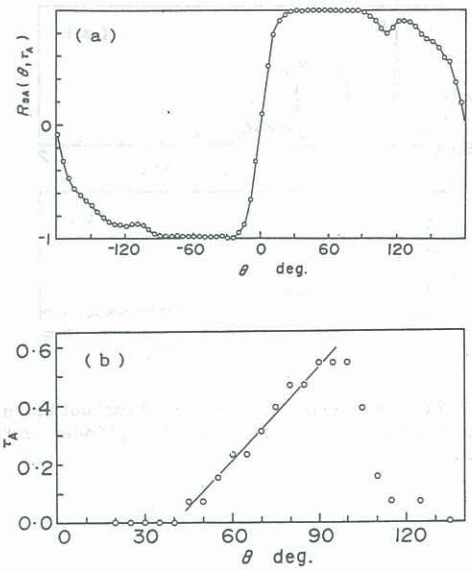

Fig. 5 Cross correlation between pressure fluctuation on surface and that at point A. (a) Cross correlation coefficient $R_a(\theta,t)$, (b) Time lag t when R_a attains maximum.

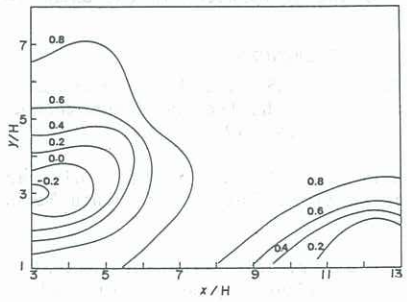

Fig. 6 Distribution of cross correlation coefficient R_b between pressure fluctuation at impinging point and that in space. Contour interval is 0.2.

Contour lines of the cross correlation coefficient $R_b(x,y,t_0)$ of the pressure fluctuation at the IP and that in space are shown in Fig. 6 for zero time lag $t_0=0$. It is remarkable that values of R_b higher than 0.8 can be seen only in a limited region except for the front and back side of the cylinder. The pressure fluctuations which produce such a high value of R_b are conjectured to be associated with the induced votex observed at phase (vii) in Fig. 2.

3.3 Acoustic intensity vector

Figure 7 shows the spatial distribution of the acoustic intensity vector around the cylinder for the fundamental frequency f_0. An arrow in Fig. 7 represents the magnitude and the direction of an acoustic intensity vector at a position of its root. The acoustic power seems to flow from the position ($x=x_e/2$, $y=H$) (source) to the separation point (sink), and to the shear layer in the vicinity of the nozzle exit (sink). It is worth noting that the IP is neither the source nor sink of the NFPF, despite that the r.m.s. surface pressure there attains the highest value. This fact means that the surface-pressure fluctuation at the IP does not propagate in space. Thus, we suppose that the pressure fluctuation propagating upstream is associated with that of the separation point.

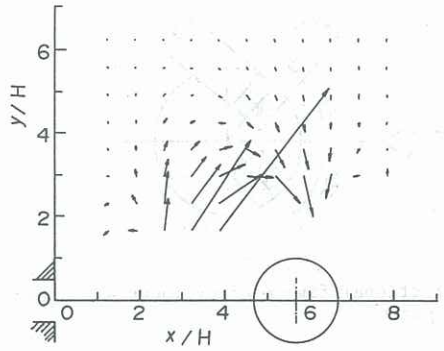

Fig. 7 Distribution of acoustic intensity vector. Arrow represent magnitude and direction of acoustic intensity at position of its root.

3.4 Reduction of NFPF

To reduce the NFPF, it is expected to be effective to prevent the upstream propagation of the pressure fluctuation. Karamcheti et al.(1965) achieved the suppression of the edge-tone by placing two plates outside of the jet, the plate being normal to the center line of the jet.

We took another approach: We intended to reduce the NFPF by suppressing the pressure fluctuation on the cylinder surface without changing the configuration of the flow field, because the pressure fluctuation propagating upstream must be produced somewhere on the cylinder. From the results of §§3.3, the positions $\theta=\pm 50$ degrees, where the large-scale vortices impinge, and the separation points $\theta=\pm 120$ degrees are expected to be an appropriate position for our purpose. A narrow region around these positions of the rigid surface of the cylinder was replaced by a low acoustic-impedance material as shown in Fig. 8.

In view of the flow of the acoustic power (Fig. 7), grooves 0.27D in width (w) and 0.3D in depth (h), which were parallel to the cylinder axis, were prepared on the cylinder at a position centered around the separation points, because we expected the pressure fluctuation propagating upstream to be produced near the separation points. The grooves were filled with a low acoustic- impedance material. However, this method was found to be ineffective in reducing the NFPF. Since the cross correlation between the pressure fluctuation at the separation point and the NFPF is smaller than that between the pressure fluctuation at the IP and the NFPF, it can be concluded that the pressure fluctuations at the separation points do not give rise to the NFPF.

The above result led to the idea that the same grooves should be put at a position centered around the IP. This turns out to be highly effective in reducing the NFPF. The reduction of 37.5dB was realized. The power spectra of the pressure fluctuation at point A with and without grooves are compared in Fig. 9. Figure 9(a) shows the spectrum for the rigid cylinder; the fundamental frequency f_0 and its harmonics are observed. Figure 9(b) clearly demonstrates not only the large reduction of the NFPF but also the disappearance of the harmonics.

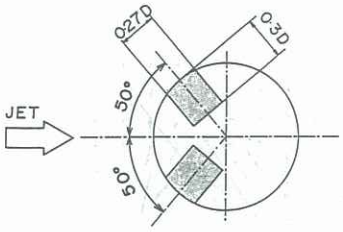

Fig. 8 Sectional figure of cylinder with grooves (shaded parts).

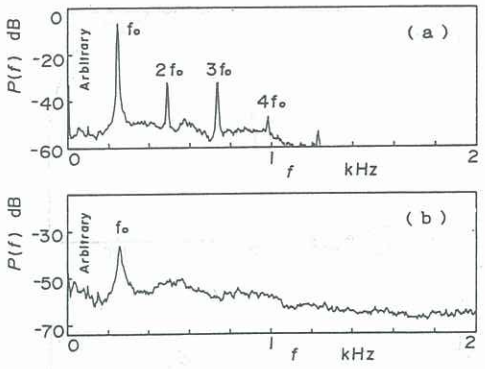

Fig. 9 Power spectrum of pressure fluctuation at point A for (a) rigid cylinder, (b) cylinder with grooves.

The disappearance of the harmonics gives a clue to understand the mechanism of the large reduction in the NFPF. Assuming that the frequency of the pressure fluctuation at the IP is equal to that of the pressure fluctuation due to the impingement of the K-H vortices, the wave length of the surface-pressure fluctuation at the IP is written as

$$l=U_c/f_v \qquad (1)$$

Here, U_c is the convection velocity of the K-H vortex and f_v denotes the frequency of the surface-pressure fluctuation due to the K-H vortices impinging on the IP. The depth h of the groove which is just to cancel the pressure fluctuation with wave length l (given by Eq. (1)) at the mouth of the groove is given by

$$h=nl/4 \qquad (2)$$

n being a positive odd integer. Equation (2) is similar to that used for the absorption of sound by a resonator. Substituting Eq. (1) into Eq. (2) to eliminate l, we obtain f_v as a function of h:

$$f_v=nU_c/(4h) \qquad (3)$$

Substituting $U_c=0.6U_0$, h=0.3D and n=1 into Eq. (3), we obtain f_v=733Hz, which is nearly equal to $3f_0$. Thus, the pressure fluctuation with the frequency $3f_0$ is effectively suppressed by the grooves. The relation $f_0=f_v/3$ is in good agreement with that between the modulating frequency component b/3 and the most unstable frequency component b of the shear layer in a self-excited planer jet impinging on a wedge (Lucas and Rockwell 1984).

Equation (3) shows that the width w of groove has little connection with the suppression of the pressure fluctuation at the IP. In order to confirm this, the NFPF generated by the cylinder having the grooves of width w/2 at the IP was measured to obtain no reduction in the NFPF. Moreover, the grooves of depth h/2 produced less reduction in the NFPF than those of depth h. These results demonstrates that Eq. (3) works well.

4. CONCLUSION

This paper has described the relation between the near-field pressure fluctuation (NFPF) produced by a two-dimentional jet impinging on a circular cylinder and the instantaneous flow fields, and an attempt to suppress NFPF by grooves made in the cylinder. Main results of the present paper can be summarized as follows.

(1) The acoustic intensity vector field was presented to identify the location of sources of the NFPF.

(2) The NFPF was well correlated with the pressure fluctuations on the surface of the cylinder.

(3) A reduction as high as 37.5dB of NFPF was realized by grooves made in the cylinder at a position where the large-scale vortices of the jet impinge. The optimum hight of the grooves was given as a function of the convection velocity and the frequency of rolling-up vortices in the shear layer of the jet.

REFERENCES

Ho, C.M. and Nosseir, N.S. (1981) Dynamics of an impinging jet. Part 1. The feedback phenomenon. J. Fluid Mech. 105, pp. 119-142.

Ho, C.M. and Huang, L.S. (1982) Subharmonics and vortex merging in mixing layers. J. Fluid Mech. 119, pp. 443-473.

Karamcheti, K., Bauer, A.B., Shields, W.L., Stegen, G.R. and Wooly, J.P. (1969) Some features of an edge-tone flow field. NASA HQ Conf., Basic Aeronaut. Noise Res., NASA Spec. Publ. 207, pp. 275-304.

Kaykayoglu, R. and Rockwell D. (1985) Vortices incident upon a leading edge: instantaneous pressure fields. J. Fluid Mech. 156, pp. 439-461.

Kaykayoglu, R. and Rockwell D. (1986) Unstable jet-edge interaction. Part 1. Instantaneous pressure fields at a single frequency. J. Fluid Mech. 169, pp. 125-149.

Lucas, M. and Rockwell, D. (1984) Self-excited jet: upstream modulation and multiple frequencies. J. Fluid Mech. 147, pp. 333-352.

Mochizuki, O. Kiya, M. and Tazumi, M. (1988) Vortex-body interaction in a jet-circular cylinder sound generating system. Fluid Dynamics Res. 3, pp.363-368.

Waser, M.P. and Crocker, M.J. (1984) Introduction to the two-microphone cross-spectral method of determining sound intensity. Noise Control Eng. J. 22-3, pp.76-85.